



**HAL**  
open science

# Assisted lipid deposition by reductive electrochemical aryldiazonium grafting and insertion of the antiport NhaA protein in this stable biomimetic membrane

T Flinois, E Lebègue, A Zebda, J-P Alcaraz, D K Martin, F Barriere

## ► To cite this version:

T Flinois, E Lebègue, A Zebda, J-P Alcaraz, D K Martin, et al.. Assisted lipid deposition by reductive electrochemical aryldiazonium grafting and insertion of the antiport NhaA protein in this stable biomimetic membrane. *Colloids and Surfaces B: Biointerfaces*, 2020, 190, pp.110924. 10.1016/j.colsurfb.2020.110924 . hal-02533167

**HAL Id: hal-02533167**

**<https://univ-rennes.hal.science/hal-02533167>**

Submitted on 7 May 2020

**HAL** is a multi-disciplinary open access archive for the deposit and dissemination of scientific research documents, whether they are published or not. The documents may come from teaching and research institutions in France or abroad, or from public or private research centers.

L'archive ouverte pluridisciplinaire **HAL**, est destinée au dépôt et à la diffusion de documents scientifiques de niveau recherche, publiés ou non, émanant des établissements d'enseignement et de recherche français ou étrangers, des laboratoires publics ou privés.

**Assisted lipid deposition by reductive electrochemical aryldiazonium grafting and insertion of the antiport NhaA protein in this stable biomimetic membrane**

T. Flinois<sup>†</sup>, E. Lebègue<sup>♣</sup>, A. Zebda<sup>‡</sup>, J.-P. Alcaraz<sup>‡</sup>, D. K. Martin<sup>‡</sup>, F. Barrière<sup>†,\*</sup>

<sup>†</sup> Univ Rennes, CNRS, Institut des Sciences Chimiques de Rennes - UMR 6226, F-35000 Rennes, France.

<sup>♣</sup> Université de Nantes, CNRS, CEISAM, UMR 6230, F-44000 Nantes, France.

<sup>‡</sup> Université Grenoble Alpes, TIMC-IMAG/CNRS/INSERM, UMR 5525, F-38000 Grenoble, France.

\*Corresponding author: [frederic.barriere@univ-rennes1.fr](mailto:frederic.barriere@univ-rennes1.fr)

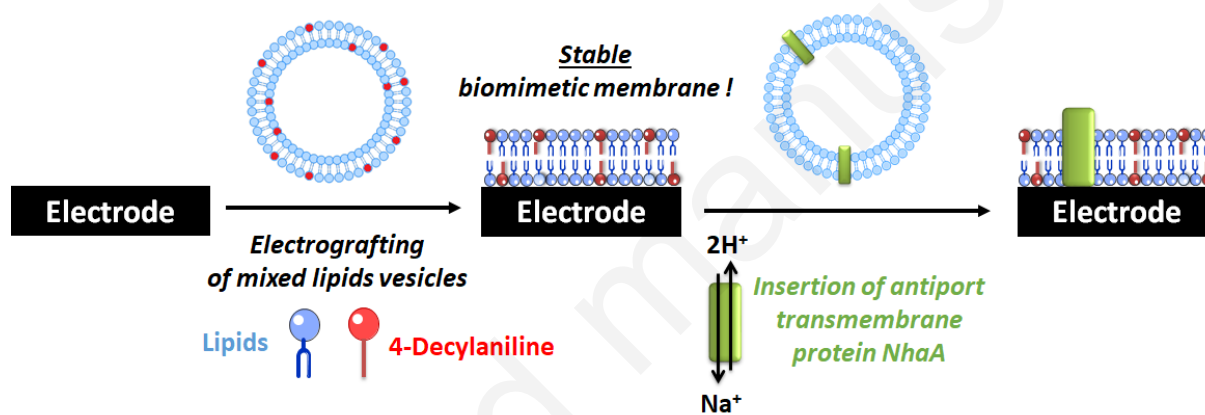
**Abstract:** Quartz crystal microbalance studies have been carried out to monitor the fusion of lipid vesicles (pure 1,2-dimyristoyl-sn-glycero-3-phosphocholine, DMPC) and mixed vesicles (DMPC and 4-decylaniline). In order to increase the stability of the lipid deposits onto the electrodes, we have developed an original approach involving electrografting of adsorbed mixed vesicles. Aryldiazonium salts generated *in situ* from 4-decylaniline (4DA) present in adsorbed and fused mixed vesicles at the electrode surface allow their cathodic reduction and subsequent grafting. The stability of the supported lipid deposit has been shown to significantly increase from less than one day for pure DMPC to about two weeks with the lipid deposition assisted by electrochemical grafting. In this stable lipid deposit, the insertion of the sodium / proton antiporter membrane protein (NhaA) or its inactive mutant has been carried out by fusion of proteoliposomes. This has been followed by characterization of the inserted protein activity by cyclic voltammetry onto an electrode previously modified by an adsorbed pH sensor (2-anthraquinone sulfonate). Activation of the protein function by sodium ions leads to a shift of the interfacial pH and confirms the integrity of the immobilized NhaA.

**Keywords:** Lipid Deposit, Antiport Protein NhaA, 4-Decylaniline, Cyclic Voltammetry, Quartz Crystal Microbalance, Electrografting

## Highlights:

- Mixed lipid vesicles containing 4-decylniline were electrografted on electrodes.
- The grafted biomimetic membrane displays an increased stability of 2 weeks.
- The antiport transmembrane protein NhaA was inserted in the stable lipid deposit.
- The function of the  $\text{Na}^+/\text{2H}^+$  antiport protein is keep intact after insertion.
- Interfacial pH change was monitored with adsorbed anthraquinone sulfonate.

## Graphical abstract:



## 1. Introduction

Biological membranes are one of Nature's most important self-assembling structures. They contain a complex and heterogeneous distribution of lipids and membrane proteins, which interact to create biological functions necessary for cell life. To study this complex membrane environment, cell membrane models are used. As opposed to natural cell membranes, these models are assembled *in vitro*. These models are used to study the fundamental properties of biological membranes in a simplified and well-controlled environment. These membranes are also implemented in biotechnological devices such as, for example, the genetic information sequencing process from Oxford Nanopore Technologies [1-2].

A model membrane can be made from a lipid deposit consisting of natural or unnatural (synthetic) lipids. The simplest model systems contain only one pure synthetic lipid. More physiologically relevant membrane bilayer models can be made with mixtures of several synthetic or natural lipids. The most common systems include lipid monolayers, lipid vesicles, lipid membranes and lipid deposits supported on a solid.

Following pioneering work by McConnell *et al.* [3] biological membrane models on solid supports have become very popular, both for the study of fundamental membrane processes and for possible biotechnological applications. Supported lipid deposits are the most commonly used models mainly because of their relative stability and robustness [4]. There are many techniques for forming supported lipid deposits such as, for example, the Langmuir-Blodgett technique [5], deposition by spin-coating [6], micro-contact printing [7], solvent exchange deposition [8], assembly induced by evaporation [9], lipid nanolithography [10], anchoring of lipids on a solid support [11], or fusion of lipid vesicles [12-17]. Fusion of lipid vesicles is relatively simple to impl simplest method and most research groups have employed this method to build supported lipid deposit. However, the stability of the formed supported lipid deposit limits the field of the applications of these method [18-21].

In this work, the adhesion and fusion of pure DMPC (1,2-dimyristoyl-sn-glycero-3-phosphocholine, Figure S1) vesicles and mixed DMPC/4DA (4-Decylaniline, Figure S1) vesicles on a gold surface has been followed with the quartz crystal microbalance. The properties of the resulting lipid deposits have been characterized by cyclic voltammetry of a redox probe (ferri-ferrocyanide) in solution. The lipid deposit obtained from mixed vesicles containing 4DA has then been electrografted to the gold surface after *in situ* generation of the corresponding aryldiazonium salt in order to produce more robust and stable lipid deposits.

The comparatively increased stability of the electrografted film has been demonstrated by monitoring the longer retention of the large peak-to-peak potential separation ( $\Delta E_p$ ) of the ferri-ferrocyanide redox probe with cyclic voltammetry. Finally, to demonstrate the usefulness of this stable biomimetic membrane, the antiport  $\text{Na}^+/2 \text{H}^+$  NhaA transmembrane protein has been integrated in the lipid deposit electrografted onto a glassy carbon electrode previously modified with an adsorbed pH sensor (anthraquinone-2-sulfonic acid, AQ) and the activity of the immobilized protein characterized.

## **2. Materials and methods**

### **2.1. Electrochemical measurements**

A three-electrode cell was used with glassy carbon or a gold disk electrode (3 mm diameter,  $0.071 \text{ cm}^2$ , IJ Cambria, UK) as the working electrode, a platinum wire as the counter electrode and an Ag/AgCl sat. KCl (BASI, USA) as the reference electrode. The working electrode was mirror-polished under a flux of ultrapure water on a fine grid silicon carbide paper from Struers (4000-grid SiC) mounted on a DAP-V Struers polishing equipment rotating at  $3.0 \times 100$  rpm then rinsed in ultrapure water before each experiment.

Electrochemical experiments were carried out at room temperature ( $21 \pm 3 \text{ }^\circ\text{C}$ ) with an Autolab AUT83857 potentiostat/galvanostat (Eco Chemie B.V., Netherlands) using Nova 2.1.1 as electrochemical software (Metrohm). Before each measurement, all solutions were deaerated by bubbling argon for at least 3 minutes. During electrochemical measurements an argon flux was kept in the electrochemical cell above the solution.

### **2.2. Chemicals and solutions**

Milli-Q water ( $18.2 \text{ M}\Omega \text{ cm}$ ) was used to prepare all solutions, lipids are obtained from Avanti Polar lipids (USA) in powder form stored in a freezer: 1,2-dimyristoyl-sn-glycero-3-phosphocholine (DMPC), 1,2-dioleoyl-sn-glycero-3-phosphocholine (DOPC) and Cardiolipin (CL). 4-Decylaniline (4DA), anthraquinone-2-sulfonic acid (AQ), sodium hydroxide, potassium hexacyanoferrate (III) and potassium hexacyanoferrate (II) trihydrate were obtained from Sigma Aldrich. Ethanol and methanol were obtained from VWR. pH of 10 mM potassium chloride (from Sigma Aldrich, USA) solution in Milli-Q water was adjusted by adding hydrochloric acid and / or sodium hydroxide. 100 mM phosphate buffer solution (pH 7) was made by dissolving 6.80 g of potassium phosphate dibasic from VWR (USA) and 7.10 g of potassium phosphate monobasic from VWR (USA) in 500 mL of Milli-Q water.

### **2.3. Preparation of liposomes, proteoliposomes and mixed vesicles**

Lipids were obtained from Avanti Polar lipids (USA) in powder form. First 6 mM of lipids (pure DMPC or lipid mixture) are dissolved in 1 mL of anhydrous ethanol. Ethanol is then evaporated under argon to obtain a lipid film. After complete ethanol evaporation, the liposomes and mixed vesicles are obtained by hydration of the lipid film. Typically, 1 mL of 10 mM phosphate buffer aqueous solution (pH 7) is added to the lipid film and the solution is placed for 5 minutes in an ultrasonic bath in order to hydrate the lipid film and to form liposomes/vesicles. The last step consists to extrude the liposome/vesicle aqueous solution in order to reach vesicles of 100 nm hydrodynamic diameter. The extrusion is carried out at  $30 \pm 5$  °C thanks to an extruder (Avanti Polar Lipids) on a hot plate. Two filtration membranes were used to obtain 100 nm diameter liposomes/vesicles (400 and 100 nm porosity "Nuclepore" polycarbonate membranes, Whatman). Table S1 compiles dynamic light scattering data for different vesicle/liposome solutions. The vesicle/liposome solutions are stored at 4 °C and used at the latest 3 days after their preparation.

Three different lipid compositions were prepared and studied: (1) the pure DMPC liposomes (100% DMPC, 6 mM), (2) the mixed DMPC/4DA vesicles containing 90% of DMPC lipids (5.4 mM) and 10% of 4DA (0.6 mM) and (3) the mixed DOPC/CL vesicles containing 75% of DOPC lipid (4.5 mM) and 25% of CL lipids (1.5 mM).

The preparation of proteoliposomes (vesicles with inserted transmembrane protein NhaA) consists to dilute the initial protein solution (0.75 mg/mL, production detailed in Section 2.6 below) in 1 mL of the mixed DOPC/CL vesicles solution previously prepared in 10 mM of phosphate buffer at pH 7 in order to reach the target protein concentration of 0.11 mg/mL. The mixed DOPC/CL vesicles solution containing 0.11 mg/mL of NhaA protein is then extruded following the extrusion procedure described above and the obtained proteoliposomes solution is also stored in fridge (4 °C) for maximum 3 days.

### **2.4. Procedure for the lipid deposit assisted by electrografting**

Prior to each lipid deposition, the gold or glassy carbon electrode is tested in a mixture of 5 mM ferricyanide and 5 mM ferrocyanide in a 10 mM potassium phosphate buffer solution at pH 7.

To form the lipid deposit, the vesicles containing 4DA and DMPC are immersed in an electrolytic solution of 10 mL of 10 mM HCl (pH 2) under argon in the presence of the electrodes (working, counter and reference). 5 mM NaNO<sub>2</sub> is added to the solution at room temperature (20 ± 3 °C). After 20 minutes, a cyclic voltammetry (generally 3 to 15 cycles for a target of total charge of 0.8 mC) is performed at 100 mV/s between +0.3 and -0.2 V vs. Ag/AgCl. After electrografting, the modified electrode was thoroughly rinsed with deionized water to remove residual adsorbents.

After or between the electrochemical characterizations, the modified electrodes are stored immersed in a solution of phosphate buffer at 100 mM pH 7 under argon at room temperature and regularly tested for stability. The stability of the lipid deposit on the electrode was evaluated by measuring the evolution of the ferricyanide redox probe  $\Delta E_p$  over time by cyclic voltammetry in phosphate buffer: When the measured delta  $E_p$  starts to decrease, the lipid membrane is considered no longer stable as its blocking properties towards the redox probe have changed and are less efficient.

## **2.5. Evaluation of the adhesion of vesicles on the surface of the gold electrode on quartz**

The influence of 4DA on the adhesion of mixed vesicles (DMPC and 4DA) was tested using quartz microbalance with frequency and resistance measurements (SE-QCA922A, from BioLogic Science Instruments). All measurements are performed at room temperature (20 ± 3 °C) on the fundamental frequency of the resonator (n=1). The electrodes used are gold-coated quartz resonators (resonance frequency 9MHz) thus forming an electrode whose projected geometric area is a 0.20 cm<sup>2</sup> disc (QA-A9M from SII).

Different concentrations of KCl in the electrolytic solution were tested: 2, 6, 8, 10, 50, 100, 200 and 300 mM. The pH of the solution with optimum KCl concentration was varied to determine the optimum pH. The pH values tested are: 1, 2, 4, 5, 7, 9.

The pH is adjusted by adding hydrochloric acid or sodium hydroxide. The liposomes are stored in a 100 mM potassium phosphate buffer solution at pH 7 and 4 °C. The conditions presented in this paper (8 to 10 mM KCl and pH 2) are optimal for observing fusion of vesicles on the gold coated resonator.

When the frequency and resistance of the gold electrode on quartz are stable, 200  $\mu\text{L}$  of liposome solution are introduced with a micropipette into the static cell to monitor their deposition and, if any, their fusion on the electrode surface.

## **2.6. Expression and purification of the NhaA transmembrane protein**

The gene of the NhaA protein is introduced into the bacterium *Escherichia coli* strain C43 by means of the plasmid vector pET15b (Novagen) in order to be overexpressed [22]. The bacteria are cultured in LB medium at 37 °C. When the absorbance at 600 nm reaches the value of 0.4, 200  $\mu\text{M}$  IPTG (Isopropyl  $\beta$ -D-1-thiogalactopyranoside) is added to the culture medium to induce overexpression of the NhaA gene. After 4 hours of culture at 37 °C, the bacteria are recovered as a pellet by centrifugation (8000 g for 10 minutes) and stored at -80°C. The purification steps consist briefly in a bacterial membrane preparation followed by detergent solubilization of membrane proteins in dodecylmaltoside and IMAC (immobilized metal affinity chromatography) purification [22]. At the end of the process, the protein concentration is adjusted at 0,75 mg/mL in elution buffer (20 mM Tris pH 7.5, 500 mM KCl, 300 mM Imidazole, 0,225 mM DDM, 10% v/v glycerol). Under these conditions, the protein is stable 2 weeks at 4 °C.

The mutant protein that can no longer be activated by sodium ions is obtained after two substitutions of nucleotides coding for amino acids. These mutations and their effects on the protein are described by Galili *et al* [23]. The DNA of the mutant protein has been cloned in pET15b and overexpress in the same manner than the native protein [22].

## **2.7. Insertion of NhaA in a lipid deposit supported on a glassy carbon electrode**

The lipid modified electrode is placed in a solution of 100 mM potassium phosphate buffer solution at pH 7 under anoxic condition (using argon) containing the proteoliposomes (with 0.11 mg/mL of protein) for 20 minutes at room temperature to allow fusion of the proteoliposomes on the lipid deposit on the electrode.

After fusion of the proteoliposomes, the electrode is again characterized by cyclic voltammetry only in a 10 mM potassium phosphate buffer solution at pH 7 before and after addition of NaCl. The 10 mM NaCl are added directly into the potassium phosphate buffer solution. The buffer solution containing the NaCl is deaerated with argon for 5 minutes before characterizing the electrode in this new electrolyte conducive to the activation of the protein.



At the end of the characterization tests, the electrode is cleaned in a solution of methanol and the washing solution (containing methanol, lipids, proteins, etc.) is stored at 4 °C to be analyzed by absorbance spectrometry at 280 nm. Optical density measurements at 280 nm verify the presence of proteins in the lipid deposit. The spectrometer used is a UV-1605 (Shimadzu), measurements are made at room temperature ( $20 \pm 3$  °C).

### 3. Results and discussion

#### 3.1. Adhesion of pure and mixed vesicles to the surface of the gold electrode

The formation of lipid deposit onto gold electrode was monitored by quartz crystal microbalance measurements (QCM). Pure DMPC liposomes can fuse to form lipid deposit on the surface of the gold electrode on quartz. The QCM results demonstrate adsorption and fusion of the DMPC vesicles (see SI, Figure S1) and are similar to those reported by Hardy *et al.* [17]. QCM measurements were also performed with mixed vesicles composed of 10 % of 4DA and 90 % DMPC (Figure 1).

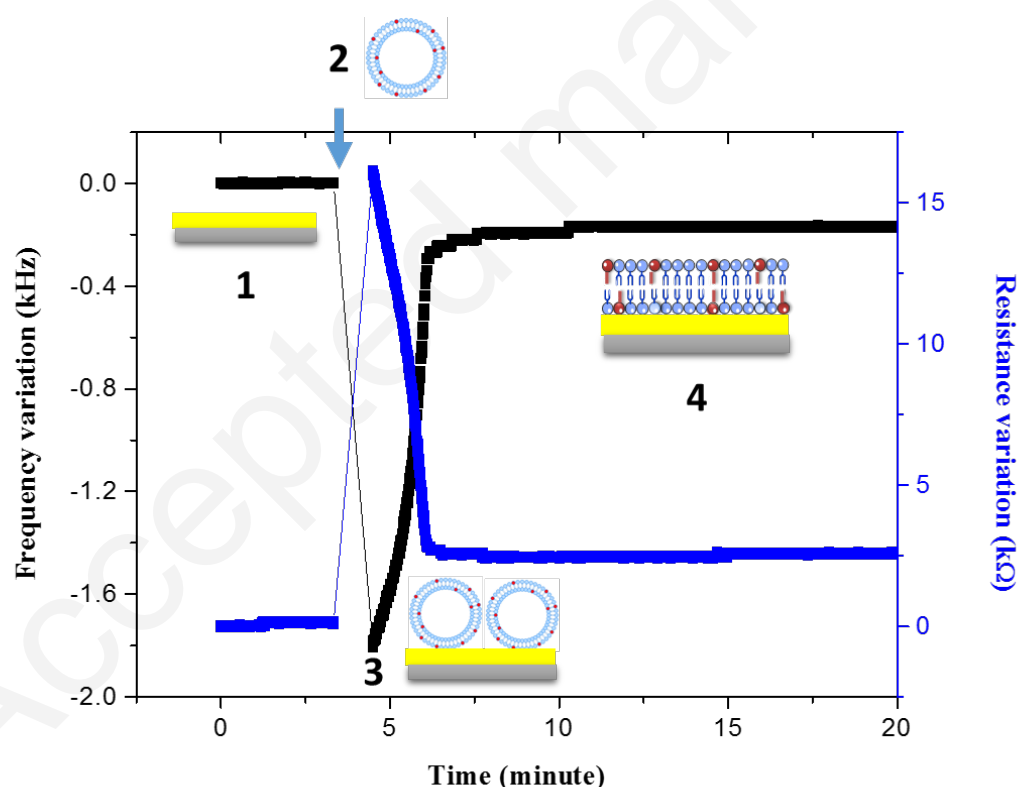


**Figure 1:** Quartz crystal microbalance results with measurement of the frequency (black) and resistance (blue) changes characterizing the fusion of mixed vesicles (90% DMPC / 10% 4DA) on a gold electrode coated on quartz in a solution of 10 mM KCl at pH 2, at 20 °C. **1.** Before addition of the vesicles **2.** Addition of mixed vesicles **3.** Rupture and fusion of the vesicles on the electrode. **4.** Formation of a lipid deposit on the electrode surface. In the

representation of the vesicles and lipid deposit the light blue color corresponds to DMPC and 4DA appears in red.

In a first step (1 in Figure 1), the electrode is in a solution of 10 mM KCl at pH 2. As soon as the vesicles are added to the quartz crystal microbalance cell (2), there is a rapid drop of the value of the frequency (mass intake) concurrent with a rapid increase in resistance (increase of the surface viscoelasticity) which corresponds to a deposit of mixed vesicles adsorbed on the surface of the electrode (3). These vesicles break up to form a rigid lipid deposit on the electrode, thus releasing their inner content. This results in an increase in frequency (mass decrease) and a decrease in resistance (relative increase of the surface viscoelasticity) (4). Using the Sauerbrey equation the frequency change after vesicles rupture and fusion compared to that of bare gold corresponds to a surface mass density in the range  $0.5$  to  $1 \mu\text{g cm}^{-2}$ .

A relatively fast (2 min) fusion of vesicles on the gold electrode is observed, Figure 1. The addition of 4DA in the composition of the vesicles does not prevent their fusion on the gold electrode surface. Cyclic voltammetry of  $5 \text{ mM K}_4\text{Fe}(\text{CN})_6 / 5 \text{ mM K}_3\text{Fe}(\text{CN})_6$  was then carried out at the modified electrode to probe its surface state (Figure 2).

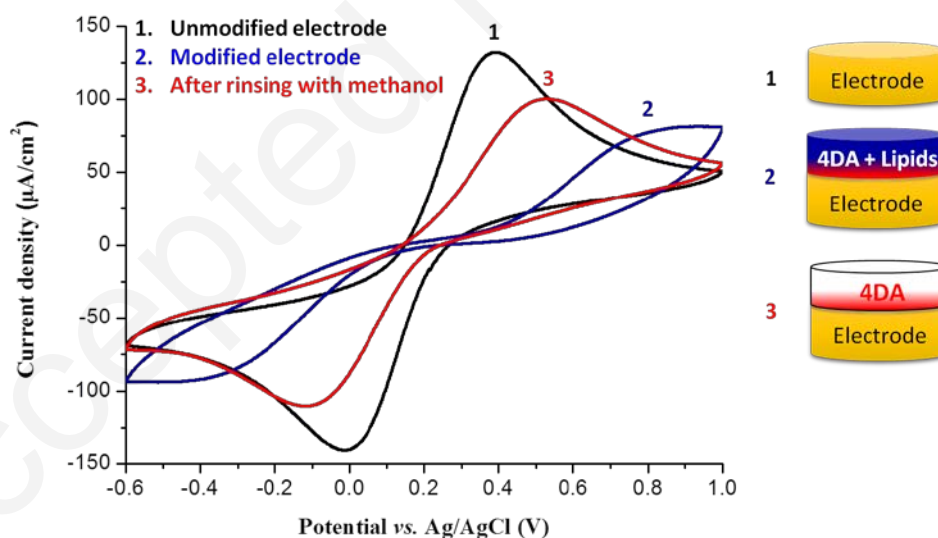


**Figure 2:** Cyclic voltammetry of  $5 \text{ mM K}_4\text{Fe}(\text{CN})_6 / 5 \text{ mM K}_3\text{Fe}(\text{CN})_6$  in  $10\text{mM KCl pH } 7$ ,  $50 \text{ mV/s}$ , under argon at 1. Unmodified gold electrode. 2. The same electrode after adsorption and fusion of the mixed vesicles. 3. After rinsing with methanol.

On the unmodified electrode, the anodic to cathodic peak potential separation for the ferri/ferrocyanide redox couple is  $\Delta E_p = 220 \text{ mV}$  and corresponds to an electrochemically quasi-reversible interfacial electron transfer. After adsorption of the mixed vesicles the peak

current density drops and  $\Delta E_p$  significantly increases to 1130 mV which indicates a significant slowdown of the electron transfer rate ascribed to the deposit of DMPC and 4DA on the electrode surface. After rinsing the electrode with methanol and removal of most of the modifiers from the surface,  $\Delta E_p$  decreases to 600 mV.

Both this larger  $\Delta E_p$  value and the lower peak current densities compared with those obtained for the unmodified electrode ( $\Delta E_p = 220$  mV) indicate that cleaning of the electrode by methanol must have been only partial.

A control experiment with pure DMPC vesicles (Figure S3) shows that the deposited lipids are nearly thoroughly washed away with methanol rinsing and indicates that 4DA is likely adsorbed more strongly to the electrode surface.

The large  $\Delta E_p$  measured (1130 mV) at the DMPC+4DA modified electrode is stable for 3 days in phosphate buffer at room temperature ( $20 \pm 3$  °C.) as opposed to only 1 day for modification with fusion of pure DMPC liposomes. Since 4DA seems more strongly adsorbed on the gold surface than DMPC alone, 4DA in mixed vesicles may serve as an efficient anchoring point slightly increasing the stability of DMPC deposited at the electrode.

Moreover, the deposited 4DA can be converted *in situ* to the corresponding aryldiazonium salt and then electro-grafted to the surface of the gold electrode. This would covalently graft the decylbenzene moiety to the gold surface and possibly further increase the stability of the DMPC lipid deposit.

The cathodic electrografting of aryldiazonium salts generated from 4DA present in the mixed vesicles and its influence on the stability of the lipid deposit are discussed next.

### **3.2. Electrografting of aryldiazonium salts generated *in situ* from 4-decylaniline in adsorbed mixed vesicles**

As discussed above, the addition of 4DA in the vesicles increases the stability of the lipid deposit at the electrode surface. It is furthermore possible to electrochemically reduce the aryldiazonium salts generated from 4DA present in the deposit and covalently graft the molecule to the gold electrode surface [24]. Molecule immobilization by cathodic reduction of aryldiazonium salts generated *in situ* is well described in the literature [25-26]. First, the *in situ* generation of 4-decyldiazonium salt from 4DA in solution has been studied. Figure S4 schematizes this procedure.

The aryldiazonium salt generated from 1 mM 4DA is obtained after incubation for 20 minutes in 10 mL 10 mM HCl (pH 2) containing 5 mM NaNO<sub>2</sub> under argon and at room temperature (20 ± 3 °C). Cyclic voltammetry (Figure 3) is carried out in the potential range +0.3 V to -0.2 V in order to avoid the oxidation of the amine group of 4DA at +0.4 V.

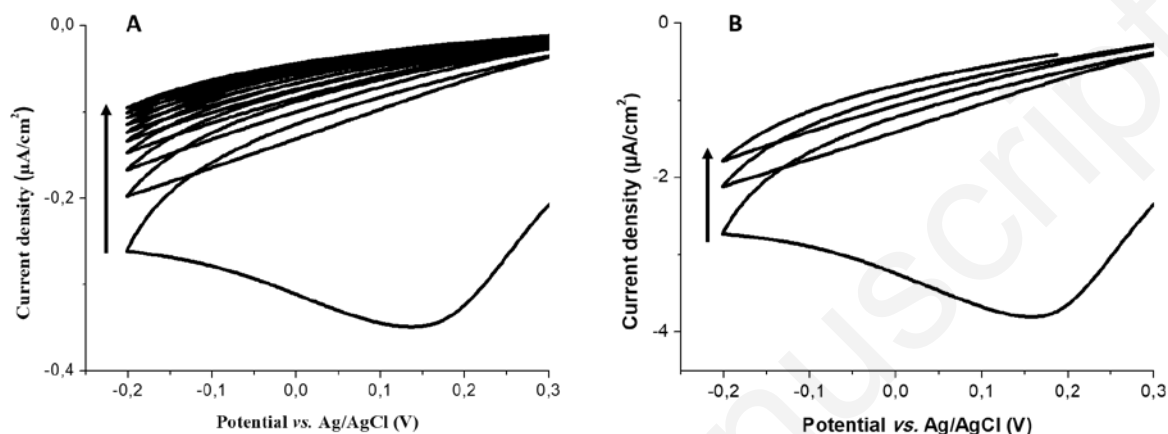


**Figure 3:** A. Voltammograms of the aryldiazonium salt generated *in situ* from 4DA into adsorbed mixed vesicles in the presence of 5 mM NaNO<sub>2</sub> in 10 mM HCl (pH 2) in the presence of 5 mM NaNO<sub>2</sub> in 10 mM HCl (pH 2) under argon. 3 cycles were carried out at 100 mV/s.

B. Voltammograms of the aryldiazonium salt generated *in situ* from 1 mM 4DA in solution and under the same conditions as Figure 3A.

During the grafting, a reduction signal at +0.17 V corresponding to the reduction of the aryldiazonium salt on the surface of the electrode is clearly visible on the first cycle of the cyclic voltammetry. As expected, [27] during the following cycles the current strongly decreases and the reduction peak of the diazonium is barely visible. This is due to molecules of decylbenzene (DB, Figure S4) already grafted on the surface and slowing down the interfacial electron transfer.

Based on this preliminary study in solution, the same procedure is applied for 4DA in vesicles adsorbed on the surface of the electrode. Figure 3A shows the voltammograms of the grafting of 4DA in adsorbed mixed vesicles (reduction peak of aryldiazonium is located at +0.14 V) and the behavior is comparable to grafting of 4DA in solution (Figure 3B) in the same conditions and the same total charged passed (0.8 mC). This demonstrates that the *in-situ* generation of aryldiazonium salts from 4DA in adsorbed mixed vesicles and its subsequent electrografting at the surface can be easily and efficiently achieved.

This modified electrode with this original lipid deposition assisted by electrochemical grafting has been electrochemically characterized in the presence of the surface sensitive ferri/ferrocyanide redox probe (Figure 4).

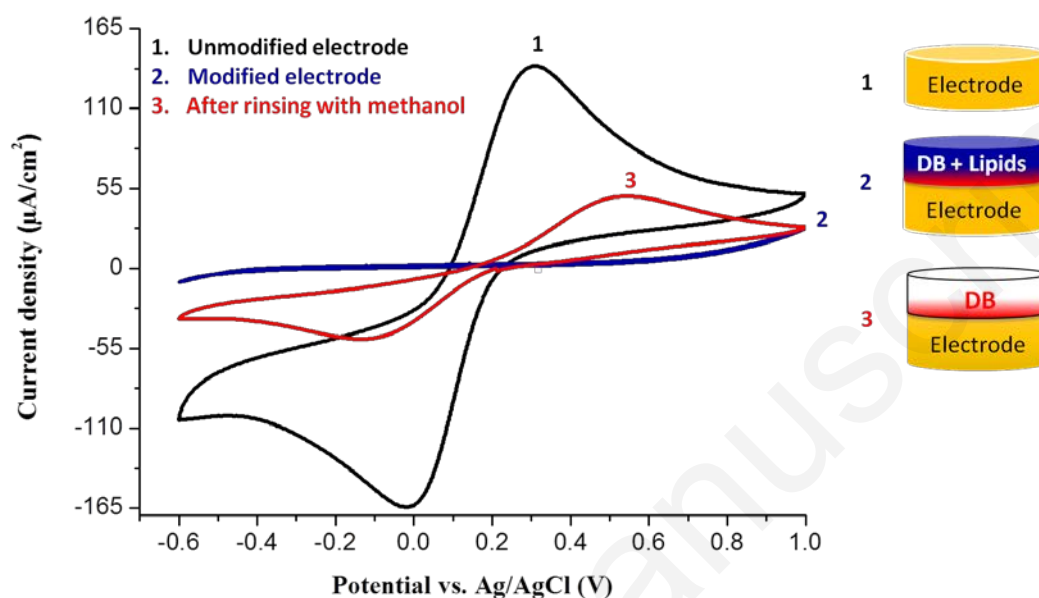


**Figure 4:** Cyclic voltammetry of 5 mM  $\text{K}_4\text{Fe}(\text{CN})_6$  / 5 mM  $\text{K}_3\text{Fe}(\text{CN})_6$  in 10 mM KCl pH 7, 50 mV/s, under argon at 1. Unmodified gold electrode. 2. The same electrode after lipid deposition assisted by electrochemical grafting. 3. After rinsing with methanol.

On the unmodified electrode, the anodic to cathodic peak potential separation for the ferri/ferrocyanide redox couple is consistently measured at  $\Delta E_p = 220$  mV and corresponds to a relatively fast and facile interfacial electron transfer (Figure 4, see also Figure 2). After lipid deposition assisted by electrochemical grafting (grafted decylbenzene (DB) + adsorbed lipids on the surface of the electrode), the redox signal of the probe is no longer observed over the range of potential studied. This loss of the redox signal of the probe indicates a significant slowdown of the interfacial electron transfer or a so called “blocking effect” of the electrode surface modification. This strongly blocking supported lipid deposit is at variance with that of the electrode only modified after the fusion of mixed vesicles where the  $\Delta E_p$  of the redox probe increased but was nevertheless still measurable (namely 1130 mV, See Figure 3). After removal of the deposit by methanol rinsing, the redox signal of the probe is again visible with  $\Delta E_p = 640$  mV, indicating a slowdown of the electron transfer induced by the remaining DB covalently attached onto the electrode surface. As a control, a gold electrode modified only by

DB with the same total charged passed (0.8 mC) during the electrografting procedure displays a similar  $\Delta E_p$  (Figure S5).

The contribution of the grafting of adsorbed 4DA on the stability of the lipid deposit supported on the electrode was then studied. The stability study consists in regularly testing the slowdown of the electronic transfer of the redox probe induced by the surface modification. If electron transfer becomes easier (*i.e.* lower  $\Delta E_p$ ), the deposition of lipids on the electrode is no longer considered stable. The results of the stability tests are compiled in Table 1 and a sample of the measurements for differently modified electrodes is provided in Figure S6.

**Table 1:** Evaluation of the stability of lipid deposit on gold electrode. 3 independent tests were performed to obtain the standard deviations.

<b>Conditions for obtaining the lipid deposit</b>	<b>Time while the blocking effect is retained</b>
<b>DMPC vesicles</b>	$1 \pm 0$ day
<b>Mixed vesicles without electrografting</b>	$3 \pm 1$ days
<b>Mixed vesicles after electrografting</b>	$14 \pm 3$ days

It is likely the lipid deposit on the gold electrode surface is stabilized through the hydrophobic interactions between the hydrocarbon chains of DMPC and that of the covalently grafted decylbenzene molecules. This deposition method seems not to be significantly impacted by the nature of the electrode surface as similar results were obtained with glassy carbon electrodes (see Figure S7 and Table S2).

In the following section we study the insertion of a transmembrane antiport protein (NhaA) in the stabilized lipid deposit and show that this original lipid deposition method may be applied for the development of interesting biomimetic membrane.

### 3.3. Insertion and detection of the $\text{Na}^+ / 2 \text{H}^+$ antiport transmembrane protein NhaA in the stabilized lipid deposit

The activity of the inserted NhaA transmembrane protein can establish a pH change at the electrode / membrane interface by transporting 1  $\text{Na}^+$  against 2  $\text{H}^+$  [28-31]. This difference in local pH can therefore in principle be detected electrochemically with immobilized molecules whose formal potential depend on pH. For this purpose, we have used adsorbed anthraquinone-2-sulfonic acid (see Figure S8 for structure) [32], thereafter named “anthraquinone” or “AQ”. AQ adsorption has been carried out on a glassy carbon electrode because its adsorption is more stable than on a gold surface. Adsorption was achieved by cycling the electrode in an AQ solution (100 mM in phosphate buffer pH 7, 10 cycles at 20 mV/s between -0.05 and -0.9 V). The apparent standard potential of AQ adsorbed on the glassy carbon electrode surface varies linearly with the pH [33-36]. (Figure 5A and 5B) with a slope of -37 mV / pH unit between pH 2 and 10.

In addition to modifying the interfacial pH, the activity of NhaA will allow ionic conductivity between the electrode and the electrolyte. The electrografting of the 4DA of the lipid deposit blocks the ionic conductivity (Figure 6), the opening of NhaA channels allowing the passage of  $\text{Na}^+$  ions and  $\text{H}^+$  thus restores the ionic conductivity.

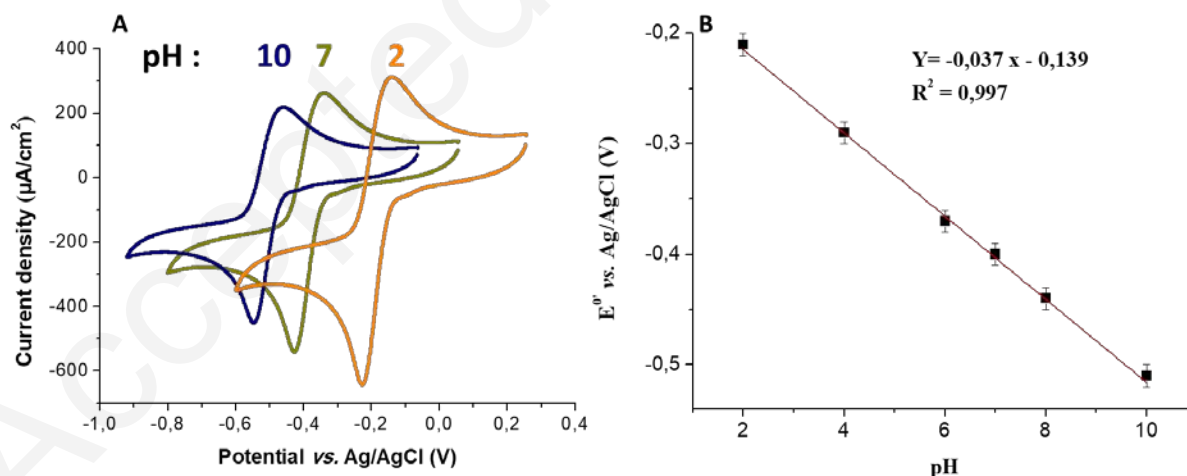


**Figure 5:** **A.** Cyclic voltammograms of the AQ-modified electrode in a solution of 10 mM KCl at pH 10 (blue), 7 (green) and 2 (orange) on a glassy carbon electrode. Scan rate 5 mV/s, under argon. **B.** Influence of pH on the apparent standard potential of the AQ-modified electrode in commercial buffered solutions, scan rate: 5 mV/s, under argon. Standard deviations are obtained through three independent tests.

After adsorption of AQ, the electrode was gently rinsed and subjected to the lipid deposition procedure assisted by electrochemical grafting and then immersed in the proteoliposome solution (*i.e.* liposomes containing the protein) for an incubation period of 20 minutes at room temperature ( $20 \pm 3$  °C) in order to insert NhaA in the stabilized lipid deposit by fusion of proteoliposomes. The composition of the proteoliposomes is a mixture of 75% of 1,2-di-(2-octadecenoyl)-sn-glycero-3-phosphocholine (DOPC,  $pK_a = 1.0$  [18]) and 25% cardiolipin (CL,  $pK_{a1} = 2.8$  and  $pK_{a2} = 7.5$  [37]), Figure S9. Proteoliposomes contain  $34 \mu\text{M}$  of DDM and  $0.11 \text{ mg/mL}$  of protein.

Thanks to the phosphate groups of cardiolipin present in the proteoliposomes, the lipid deposit is now negatively charged at pH 7 [38]. A charged lipid deposit is important to avoid its instability induced by the addition of sodium ions (by adding sodium chloride) as in the case of pure DMPC (zwitterionic) lipid deposit [39].

This is here especially critical here because the activation of the inserted protein and consequently the restauration of the ionic current at the lipid/electrode interface are triggered by addition of  $\text{Na}^+$  ions.

Figure 6 presents the voltammogram obtained before deposition of the lipids (black curve). The redox signals of AQ adsorbed on the surface of the electrode are visible and correspond to a solution of pH 7, *i.e.* the pH of the electrolyte. As a result of lipid deposition assisted by electrografting and subsequent fusion of proteoliposomes, the redox signals of the adsorbed AQ are no longer visible (blue curve). This is ascribed to the blocking of the ionic current by the biomimetic membrane showing that the lipid deposition mimics the impermeability of biological membrane *vis-à-vis* protons and other ions. A sharp drop in the capacitive current is also observed, confirming the loss of the ionic current between the electrode and the electrolyte.

After addition of  $10 \text{ mM}$  NaCl in the KCl pH 7 electrolyte, the redox signals of AQ are again visible (Figure 6, red curve). The addition of sodium ion allows the activation of the protein through the opening of its proton and sodium exchange channels, thus restoring the ionic current at the modified electrode / lipid deposit interface.



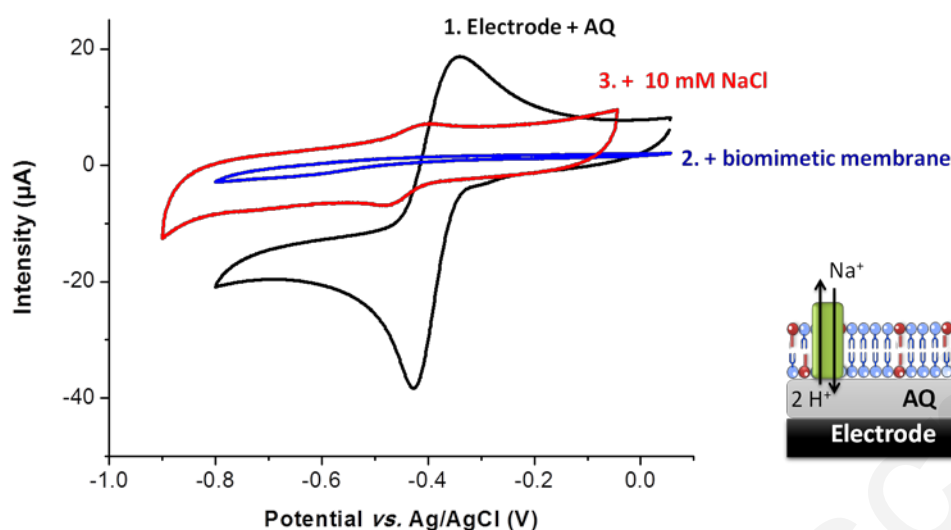


**Figure 6:** 1. Cyclic voltammograms of the anthraquinone (AQ) adsorbed on glassy carbon electrode. 2 after deposition of lipids and fusion of proteoliposomes containing the native protein. 3. after activation of the protein following the addition of 10 mM NaCl in the electrolyte. Scan rate: 20 mV/s. All measurements are performed under argon and in a 10 mM KCl solution initially at pH 7.

In addition, one notes that the capacitive current is identical to that of the electrode before deposition of the membrane indicating a restoration of the ionic current between the electrode and the electrolyte. The recovery of ionic current following activation of NhaA by sodium chloride addition is consistent with observations made in the literature on various ion transporters inserted into biomimetic membranes [40-43].

It is also noted that the apparent standard potential of adsorbed AQs at the surface of the electrode shifts by -37 mV after sodium chloride addition which corresponds to local change in pH at the electrode / lipid deposit interface from pH 7 (pH 7 of the electrolyte) to pH 8.

The restoration of the ionic current and the change of pH at the electrode / lipid deposit interface indicate that the lipid deposit supported at the electrode allows the insertion of NhaA without altering its  $\text{Na}^+ / 2 \text{H}^+$  antiport function.

As a negative control, a test was performed with a mutant NhaA protein that can no longer be activated by sodium ions. In this case and after addition of 10 mM NaCl, no redox signal is detected in the voltammogram (Figure S10), contrary to the experiment reported in Figure 7 with the native protein.

This indicates that the channels of the mutant protein are not open and is consistent with the mutation applied to render the protein insensitive to the presence of sodium ions.

In order to verify that the native or mutant NhaA protein are well inserted into the lipid deposit as a result of fusion of the proteoliposomes, the lipid deposit on the surface of the electrodes were recovered by methanol washing to measure the absorbance at 280 nm [44]. Absorbance measurements at 280 nm (Table S3) were performed in 1 mL of lipid-containing methanol washing solution (DMPC, DOPC, CL) and possibly proteins.

The sample obtained after cleaning the electrode containing only the lipid deposit does not absorb at 280 nm and is fully consistent with the absence of protein at the electrode. Samples containing NhaA (native or mutant) absorb at 280 nm and confirm the presence of the transmembrane protein in the lipid deposit. The cyclic voltammetry studies discussed above, and the spectroscopic measurements indicate that the lipid deposition assisted by electrografting onto a glassy carbon electrode modified by adsorbed pH responsive AQ molecules allow the insertion of the NhaA transmembrane protein without altering its  $\text{Na}^+ / 2 \text{H}^+$  antiport function.

#### **4. Conclusions and perspectives**

The electrografting of aryldiazonium generated from 4DA in mixed vesicles also containing DMPC is readily achieved and yields lipid deposits with a markedly increased stability (2 weeks *vs* less than one day for pure DMPC). The insertion of a functional biological ion transporter in this stabilized lipid deposit has been demonstrated with the  $\text{Na}^+ / 2 \text{H}^+$  antiport transmembrane NhaA protein.

In this study, the 4DA / DMPC ratio is 10% 4DA for 90% DMPC. It would be interesting to modify this ratio in order to optimize the lipid anchoring effect of electrografting.

In addition, the mixed vesicles have been prepared with 4DA present both on the inner and the outer side of the vesicles, they are said to be symmetrical. Controlling the distribution of 4DA and obtaining asymmetric vesicles (4DA only on the outside of the vesicles) [45] would optimize the amount of 4DA prone to electrografting on the electrode. Finally, directly using mixed vesicles comprising the protein to be deposited on the electrode would be an interesting alternative to the present procedure.

## Acknowledgements

The authors thank the ANR-15-CE05-0003 bioWATTS project for financial support.

## References

- [1] N.J. Loman, M. Watson, Successful test launch for nanopore sequencing, *Nature Methods*. 12 (2015) 303–304. doi:10.1038/nmeth.3327.
- [2] A.S. Mikheyev, M.M.Y. Tin, A first look at the Oxford Nanopore MinION sequencer, *Molecular Ecology Resources*. 14 (2014) 1097–1102. doi:10.1111/1755-0998.12324.
- [3] H.M. McConnell, T.H. Watts, R.M. Weis, A.A. Brian, Supported planar membranes in studies of cell-cell recognition in the immune system, *Biochim. Biophys. Acta*. 864 (1986) 95–106. doi:10.1016/0304-4157(86)90016-x
- [4] E.T. Castellana, P.S. Cremer, Solid supported lipid bilayers: From biophysical studies to sensor design, *Surface Science Reports*. 61 (2006) 429–444. doi:10.1016/j.surfrep.2006.06.001.
- [5] L.K. Tamm, H.M. McConnell, Supported phospholipid bilayers, *Biophysical Journal*. 47 (1985) 105–113. doi:10.1016/S0006-3495(85)83882-0.
- [6] U. Mennicke, T. Salditt, Preparation of Solid-Supported Lipid Bilayers by Spin-Coating, *Langmuir*. 18 (2002) 8172–8177. doi:10.1021/la025863f.
- [7] S.-Y. Jung, M.A. Holden, P.S. Cremer, C.P. Collier, Two-component membrane lithography via lipid backfilling, *Chemphyschem*. 6 (2005) 423–426. doi:10.1002/cphc.200400540.
- [8] A.O. Hohner, M.P.C. David, J.O. Rädler, Controlled solvent-exchange deposition of phospholipid membranes onto solid surfaces, *Biointerphases*. 5 (2010) 1–8. doi:10.1116/1.3319326.
- [9] C.J. Brinker, Y. Lu, A. Sellinger, H. Fan, Evaporation-Induced Self-Assembly: Nanostructures Made Easy, *Advanced Materials*. 11 (1999) 579–585. doi:10.1002/(SICI)1521-4095(199905)11:7<579:AID-ADMA579>3.0.CO;2-R.
- [10] S. Lenhart, C.A. Mirkin, H. Fuchs, In situ lipid dip-pen nanolithography under water, *Scanning*. 32 (2010) 15–23. doi:10.1002/sca.20166.
- [11] H. Lang, C. Duschl, H. Vogel, A new class of thiolipids for the attachment of lipid bilayers on gold surfaces, *Langmuir*. 10 (1994) 197–210. doi:10.1021/la00013a029.
- [12] G.J. Hardy, R. Nayak, S. Zauscher, Model cell membranes: Techniques to form complex biomimetic supported lipid bilayers via vesicle fusion, *Curr Opin Colloid Interface Sci*. 18 (2013) 448–458. doi:10.1016/j.cocis.2013.06.004.
- [13] H. Egawa, K. Furusawa, Liposome Adhesion on Mica Surface Studied by Atomic Force Microscopy, *Langmuir*. 15 (1999) 1660–1666. doi:10.1021/la980923w.
- [14] R. Richter, A. Mukhopadhyay, A. Brisson, Pathways of Lipid Vesicle Deposition on Solid Surfaces: A Combined QCM-D and AFM Study, *Biophysical Journal*. 85 (2003) 3035–3047. doi:10.1016/S0006-3495(03)74722-5.
- [15] R.P. Richter, R. Bérat, A.R. Brisson, Formation of Solid-Supported Lipid Bilayers: An Integrated View, *Langmuir*. 22 (2006) 3497–3505. doi:10.1021/la052687c.
- [16] D. Stroumpoulis, A. Parra, M. Tirrell, A kinetic study of vesicle fusion on silicon dioxide surfaces by ellipsometry, *AIChE Journal*. 52 (2006) 2931–2937. doi:10.1002/aic.10914.

- [17] G.J. Hardy, R. Nayak, S.M. Alam, J.G. Shapter, F. Heinrich, S. Zauscher, Biomimetic supported lipid bilayers with high cholesterol content formed by  $\alpha$ -helical peptide-induced vesicle fusion, *J Mater Chem.* 22 (2012) 19506–19513. doi:10.1039/C2JM32016A.
- [18] F.C. Tsui, D.M. Ojcius, W.L. Hubbell, The intrinsic pKa values for phosphatidylserine and phosphatidylethanolamine in phosphatidylcholine host bilayers, *Biophys. J.* 49 (1986) 459–468. doi:10.1016/S0006-3495(86)83655-4.
- [19] D.-W. Jeong, H. Jang, S.Q. Choi, M.C. Choi, Enhanced stability of freestanding lipid bilayer and its stability criteria, *Scientific Reports.* 6 (2016). doi:10.1038/srep38158.
- [20] M. Snejdárková, M. Reháč, M. Otto, Stability of bilayer lipid membranes on different metallic supports, *Biosens Bioelectron.* 12 (1997) 145–153. doi: 10.1016/S0956-5663(97)87060-1
- [21] D.S. Dimitrov, R.K. Jain, Membrane stability, *Biochimica et Biophysica Acta (BBA) - Reviews on Biomembranes.* 779 (1984) 437–468. doi:10.1016/0304-4157(84)90020-0.
- [22] J.P. Alcaraz, PhD thesis, Université Grenoble Alpes, 2016.
- [23] L. Galili, K. Herz, O. Dym, E. Padan, Unraveling functional and structural interactions between transmembrane domains IV and XI of NhaA Na<sup>+</sup>/H<sup>+</sup> antiporter of *Escherichia coli*, *J. Biol. Chem.* 279 (2004) 23104–23113. doi:10.1074/jbc.M400288200.
- [24] L. Laurentius, S.R. Stoyanov, S. Gusarov, A. Kovalenko, R. Du, G.P. Lopinski, M.T. McDermott, Diazonium-Derived Aryl Films on Gold Nanoparticles: Evidence for a Carbon–Gold Covalent Bond, *ACS Nano.* 5 (2011) 4219–4227. doi:10.1021/nn201110r.
- [25] D. Bélanger, J. Pinson, Electrografting: a powerful method for surface modification, *Chemical Society Reviews.* 40 (2011) 3995. doi:10.1039/c0cs00149j.
- [26] F. Barrière, A.J. Downard, Covalent modification of graphitic carbon substrates by non-electrochemical methods, *Journal of Solid State Electrochemistry.* 12 (2008) 1231–1244. doi:10.1007/s10008-008-0526-2.
- [27] S. Lin, C.-W. Lin, J.-H. Jhang, W.-H. Hung, Electrodeposition of Long-Chain Alkylaryl Layers on Au Surfaces, *The Journal of Physical Chemistry C.* 116 (2012) 17048–17054. doi:10.1021/jp304502e.
- [28] D. Taglicht, E. Padan, S. Schuldiner, Overproduction and purification of a functional Na<sup>+</sup>/H<sup>+</sup> antiporter coded by nhaA (ant) from *Escherichia coli*, *J. Biol. Chem.* 266 (1991) 11289–11294. PMID:1645730
- [29] D. Taglicht, E. Padan, S. Schuldiner, Proton-sodium stoichiometry of NhaA, an electrogenic antiporter from *Escherichia coli.*, *J. Biol. Chem.* 268 (1993) 5382–5387. PMID:8383669
- [30] M. Venturi, E. Padan, Purification of NhaA Na<sup>+</sup>/H<sup>+</sup> Antiporter of *Escherichia coli* for 3D or 2D Crystallization, in: *Membrane Protein Purification and Crystallization*, Elsevier, 2003: pp. 179–190. doi:10.1016/B978-012361776-7/50011-5.
- [31] Y. Huang, W. Chen, D.L. Dotson, O. Beckstein, J. Shen, Mechanism of pH-dependent activation of the sodium-proton antiporter NhaA, *Nature Communications.* 7 (2016) 12940. doi:10.1038/ncomms12940.
- [32] C. Batchelor-McAuley, B.R. Kozub, D. Menshkykau, R.G. Compton, Voltammetric Responses of Surface-Bound and Solution-Phase Anthraquinone Moieties in the Presence of Unbuffered Aqueous Media, *J. Phys. Chem. C.* 115 (2011) 714–718. doi:10.1021/jp1096585.

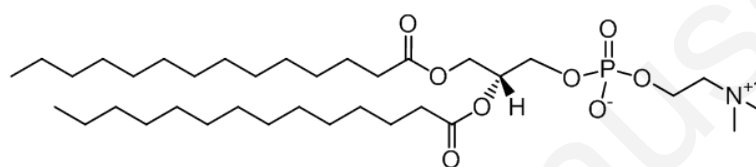
- [33] J.J. Hickman, D. Ofer, P.E. Laibinis, G.M. Whitesides, M.S. Wrighton, Molecular Self-Assembly of Two-Terminal, Voltammetric Microsensors with Internal References, *Science*. 252 (1991) 688–691. doi:10.1126/science.252.5006.688.
- [34] G. Wildgoose, Anthraquinone-derivatised carbon powder: reagentless voltammetric pH electrodes, *Talanta*. 60 (2003) 887–893. doi:10.1016/S0039-9140(03)00150-4.
- [35] H. Leventis, Derivatised carbon powder electrodes: reagentless pH sensors, *Talanta*. 63 (2004) 1039–1051. doi:10.1016/j.talanta.2004.01.017.
- [36] I. Streeter, H.C. Leventis, G.G. Wildgoose, M. Pandurangappa, N.S. Lawrence, L. Jiang, T.G.J. Jones, R.G. Compton, A sensitive reagentless pH probe with a ca. 120mV/pH unit response, *Journal of Solid-State Electrochemistry*. 8 (2004). doi:10.1007/s10008-004-0536-7.
- [37] G. Olofsson, E. Sparr, Ionization Constants pKa of Cardiolipin, *PLOS ONE*. 8 (2013) e73040. doi:10.1371/journal.pone.0073040.
- [38] D. Marsh, Thermodynamics of Phospholipid Self-Assembly, *Biophysical Journal*. 102 (2012) 1079–1087. doi:10.1016/j.bpj.2012.01.049.
- [39] R.A. Böckmann, A. Hac, T. Heimbürg, H. Grubmüller, Effect of Sodium Chloride on a Lipid Bilayer, *Biophysical Journal*. 85 (2003) 1647–1655. doi:10.1016/S0006-3495(03)74594-9.
- [40] M. Inabayashi, S. Miyauchi, N. Kamo, T. Jin, Conductance Change in Phospholipid Bilayer Membrane by an Electroneutral Ionophore, Monensin, *Biochemistry*. 34 (1995) 3455–3460. doi:10.1021/bi00010a038.
- [41] S. Maher, H. Basit, R.J. Forster, T.E. Keyes, Micron dimensioned cavity array supported lipid bilayers for the electrochemical investigation of ionophore activity, *Bioelectrochemistry*. 112 (2016) 16–23. doi:10.1016/j.bioelechem.2016.07.002.
- [42] G. Stark, B. Ketterer, R. Benz, P. Läger, The Rate Constants of Valinomycin-Mediated Ion Transport through Thin Lipid Membranes, *Biophysical Journal*. 11 (1971) 981–994. doi:10.1016/S0006-3495(71)86272-0.
- [43] C. Steinem, A. Janshoff, K. von dem Bruch, Karsten Reihls, J. Goossens, H.-J. Galla, Valinomycin-mediated transport of alkali cations through solid supported membranes, *Bioelectrochemistry and Bioenergetics*. 45 (1998) 17–26. doi:10.1016/S0302-4598(98)00073-7.
- [44] E. Layne, Spectrophotometric and turbidimetric methods for measuring proteins, in: *Methods in Enzymology*, Elsevier, 1957: pp. 447–454. doi:10.1016/S0076-6879(57)03413-8.
- [45] S. Pautot, B.J. Frisken, D.A. Weitz, Engineering asymmetric vesicles, *Proceedings of the National Academy of Sciences*. 100 (2003) 10718–10721. doi:10.1073/pnas.1931005100.

## SUPPORTING INFORMATION

### Assisted lipid deposition by reductive electrochemical aryldiazonium grafting and insertion of the antiport NhaA protein in this stable biomimetic membrane

T. Flinois<sup>†</sup>, E. Lebègue<sup>‡</sup>, A. Zebda<sup>‡</sup>, J.-P. Alcaraz<sup>‡</sup>, D. K. Martin<sup>‡</sup>, F. Barrière<sup>†,\*</sup>

\*Corresponding author: [frederic.barriere@univ-rennes1.fr](mailto:frederic.barriere@univ-rennes1.fr)



1,2-dioleoyl-sn-glycero-3-phosphocholine



4-decylaniline

**Figure S1:** Molecular structures of 1,2-dimyristoyl-sn-glycero-3-phosphocholine (DMPC) and 4-decylaniline (4DA).

**Table S1:** Dynamic light scattering measurements and estimated hydrodynamic diameter of vesicles and proteoliposomes formed by extrusion.

Vesicles and proteoliposomes	Diameter (nm)	Standard deviation (%)	Polydispersity Index
DMPC	104	24	0.12
DMPC + 4DA	117	31	0.09
DOPC + CL + Native-NhaA	135	47	0.22
DOPC + CL + Mutant-NhaA	130	53	0.28

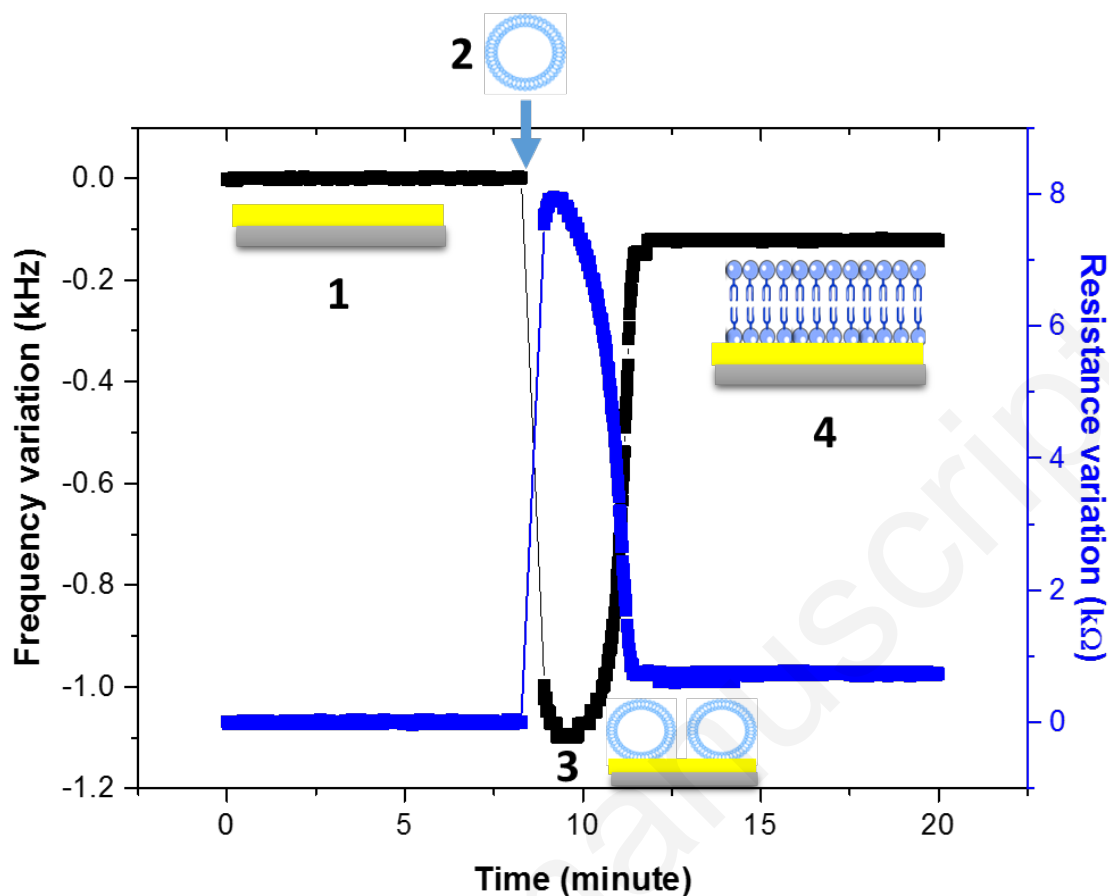


**Figure S2:** Quartz crystal microbalance results with measurement of the frequency (black) and resistance (blue) changes characterizing the fusion of pure DMPC vesicles on a gold electrode coated on quartz in a solution of 10 mM KCl at pH 2, at 20 °C. **1.** Before addition of the vesicles **2.** Addition of DMPC vesicles **3.** Rupture and fusion of the vesicles on the electrode **4.** Formation of a lipid deposit on the electrode surface. In the representation of the vesicles and lipid deposit the light blue color corresponds to DMPC.

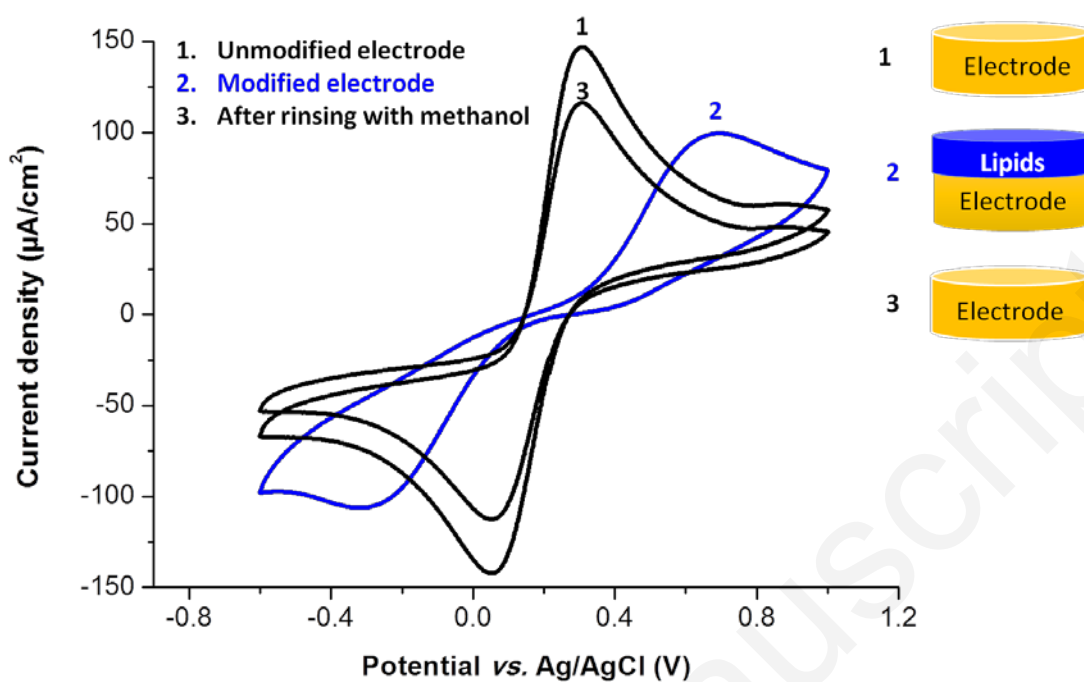


**Figure S3:** Cyclic voltammetry of 5 mM  $\text{K}_4\text{Fe}(\text{CN})_6$  / 5 mM  $\text{K}_3\text{Fe}(\text{CN})_6$  in 10 mM KCl pH 7, 50 mV/s, under argon at **1.** Unmodified gold electrode. **2.** The same electrode after depositing the DMPC vesicles. **3.** After rinsing with methanol.



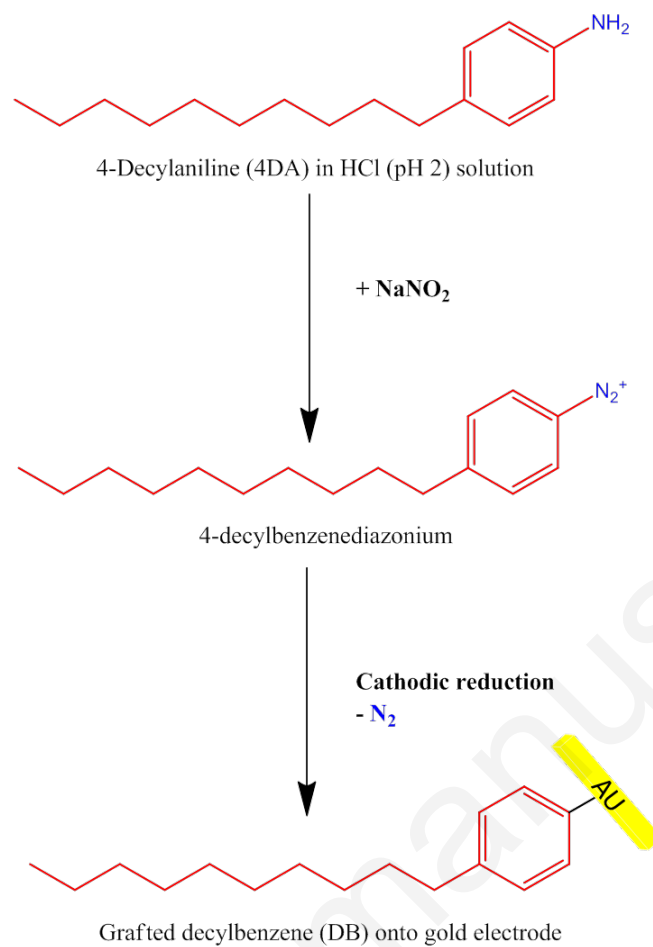


**Figure S4:** Steps implemented during electrografting of aryldiazonium salt generated *in situ* from 4DA in solution on the surface of the gold electrode.

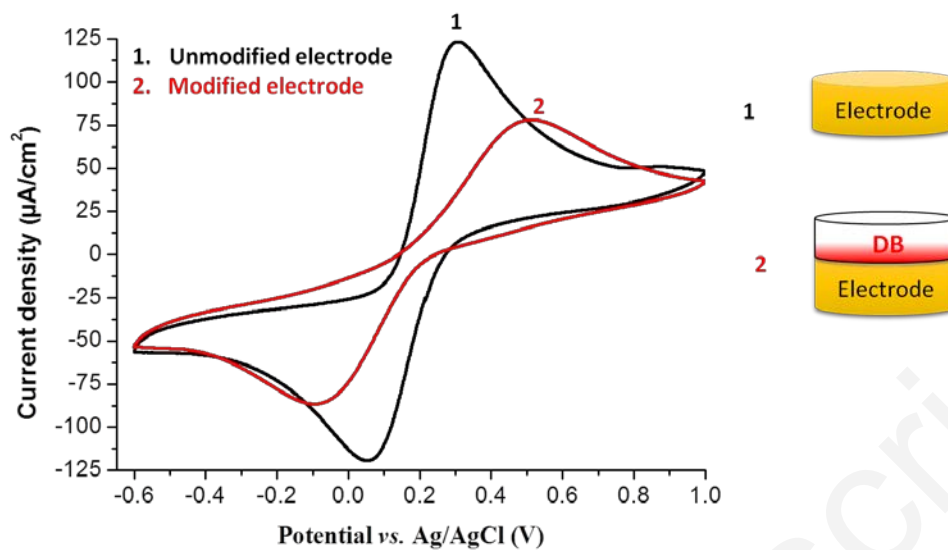


**Figure S5:** Cyclic voltammetry of 5 mM  $\text{K}_4\text{Fe}(\text{CN})_6$  / 5 mM  $\text{K}_3\text{Fe}(\text{CN})_6$  in 10 mM KCl pH 7, 50 mV/s, under argon at **1**. Unmodified gold electrode. **2**. The same electrode after electrografting of 4DA (DB).

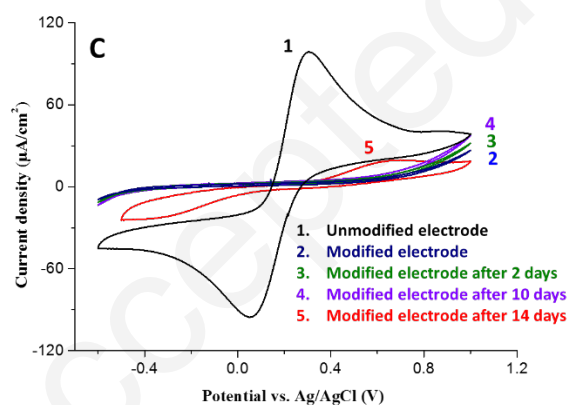
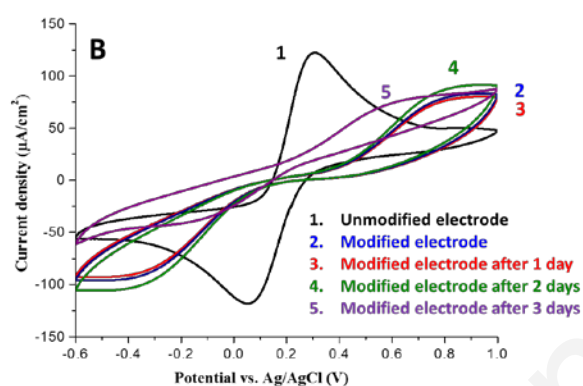
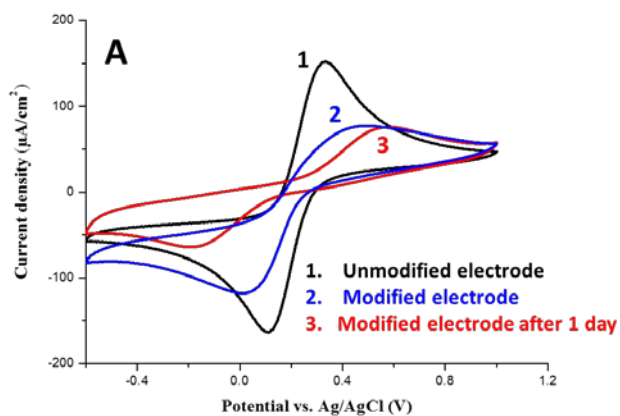


**Figure S6:** Samples of the monitoring of ferri-ferrocyanide delta  $E_p$  over time with cyclic voltammetry for assessing the stability of the lipid deposit on a gold electrode.

Conditions: 5 mM  $\text{K}_4\text{Fe}(\text{CN})_6$  / 5 mM  $\text{K}_3\text{Fe}(\text{CN})_6$  in 10 mM KCl pH 7, 50 mV/s, under argon.

Nature of the lipid deposit: pure DMPC (A), Mixed DMPC and 4DA (B) and Mixed DMPC and 4DA followed by electrografting (C).

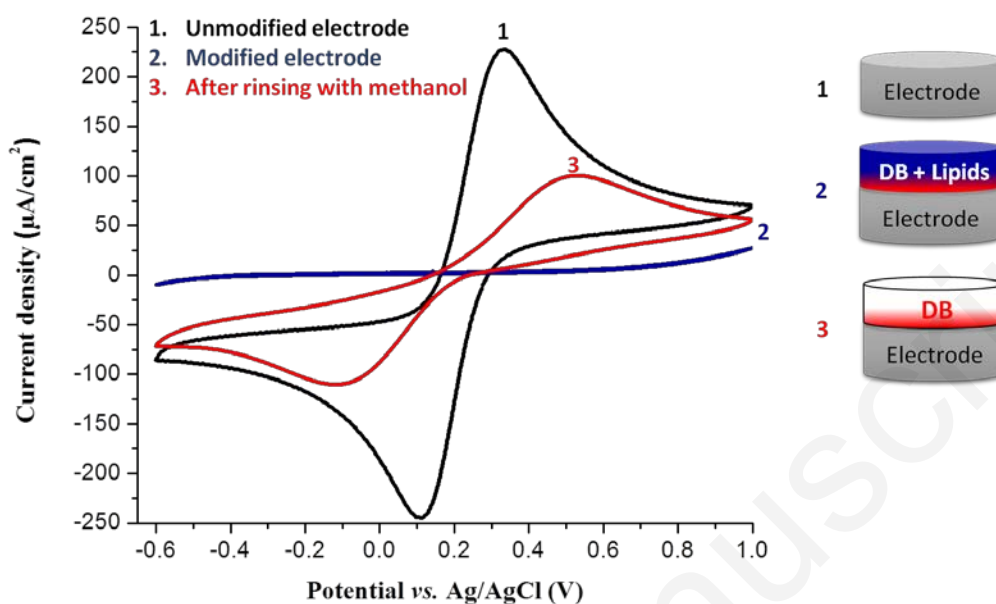


**Figure S7:** Cyclic voltammetry of 5 mM  $K_4Fe(CN)_6$  / 5mM  $K_3Fe(CN)_6$  in 10 mM KCl pH 7, 50 mV/s, under argon at **1**. Unmodified glassy carbon electrode. **2**. The same electrode after lipid deposition assisted by electrochemical grafting. **3**. After rinsing with methanol.

**Table S2:** Evaluation of the stability of lipid deposit on glassy carbon electrode. 3 independent tests were performed to obtain the standard deviations.

Conditions for obtaining the lipid deposit	Time while the blocking effect is retained
DMPC vesicles	$2 \pm 1$ days
Mixed vesicles without electrografting	$4 \pm 1$ days
Mixed vesicles after electrografting	$14 \pm 2$ days

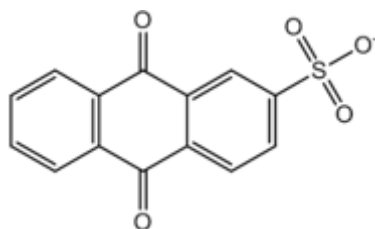
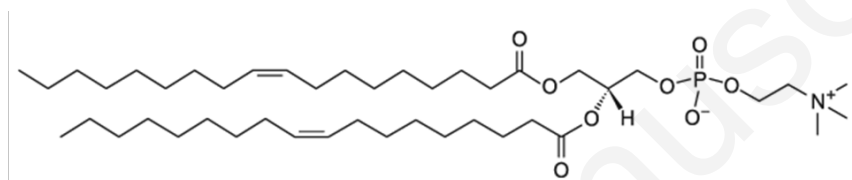
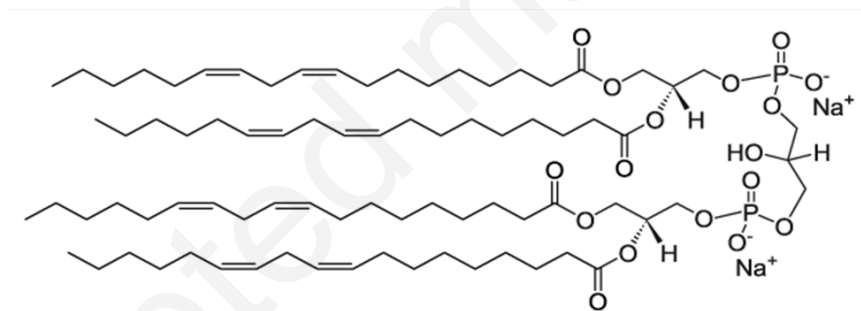


**Figure S8:** Molecular structure of anthraquinone-2-sulfonic acid (AQ).



1,2-dioleoyl-sn-glycero-3-phosphocholine (DOPC)



Cardiolipin (CL)

**Figure S9:** Molecular structure of the lipids (DOPC and CL) composing the proteoliposomes used for the insertion of the transmembrane antiport NhaA.

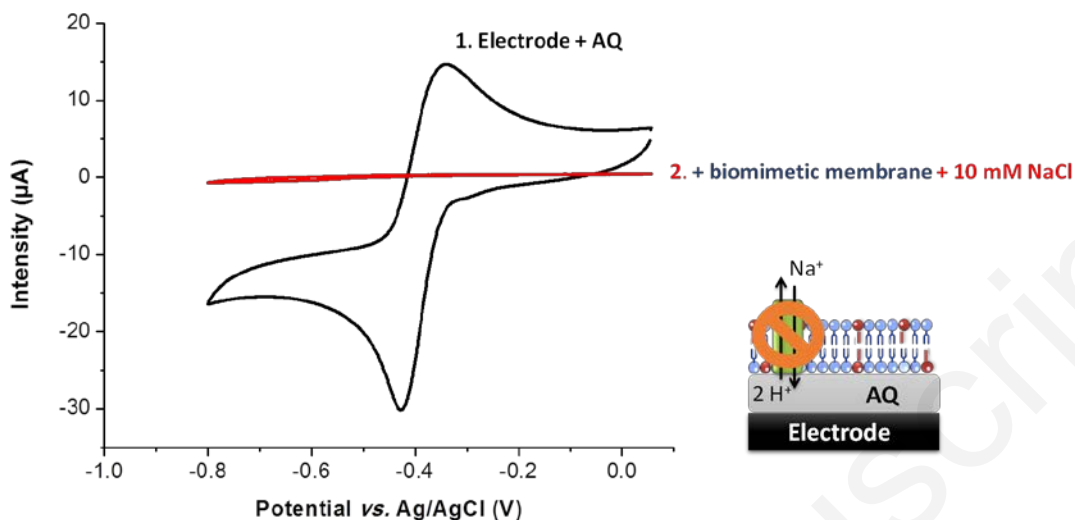


**Figure S10. 1.** Cyclic voltammogram of the electrode modified by anthraquinone (AQ) adsorbed on its surface. 2. Voltammogram obtained after the formation of the biomimetic membrane and addition of 10 mM NaCl in the electrolyte: the mutant protein cannot be activated by  $\text{Na}^+$  and the restoration of the redox signals of AQs is not observed. Scan rate: 20 mV/s. All measurements are performed under argon and in a solution of 10 mM KCl at initially pH 7.

**Table S3:** Absorbance at 280 nm measured from various solutions of lipid deposit recovery supported on an electrode. 3 independent samples were tested to obtain standard deviations. Measurements were made at room temperature and under air. The reference solution contains DMPC, DOPC and CL in 1 mL of methanol.

Sample	Absorbance at 280 nm
Liposomes	0.000 ± 0.000
Native NhaA	0.121 ± 0.035
Mutant NhaA	0.110 ± 0.027